Material Science Research India Vol. **6**(1), 53-61 (2009)

Conduction and solid state battery characteristic studies of AgI-Ag_2O-P_2O_5-Fe_2O_3 glass

FATHY SALMAN[1], MABROUK EL-MANSY[1], AHMAD MOSTAFA[2] and HANY HAZZAA[1]

[1]Faculty of Science, Benha University, Benha (Egypt).
[2]Faculty of Science, Al-Azhar University, Nasr City (Egypt).

(Received: March 03, 2009; Accepted: April 30, 2009)

ABSTRACT

Various compositions of silver-based superionic conducting [AgI – Ag_2O-P_2O_5-Fe_2O_3] glasses were prepared by melt quenching technique. X-ray diffraction (XRD),Mossbauer effect (ME), infrared (IR), differential thermal analysis (DTA) and electrical conductivity studies were carried out to optimize the high ionic conducting composition. Solid-State primary batteries were fabricated using the $20P_2O_5$-$30AgI$-$40Ag_2O$-$10Fe_2O_3$ glass with Ag_2S as anode and Ag as cathode of type; ((Ag_2S + SE) / solid electrolyte / Ag). Superionic solid electrolyte glass for rechargeable battery application was performed and characterized at many conditions such as different thichnesses , different pressures , different load resistance , different temperatures , annealing times and different storage times.

Key words: Conduction and solid state battery characteristic studies.

INTRODUCTION

Superionic conducting glass are of technological significance because of their application in solid state batteries, other ionic devices, etc., at ambient temperature[1-3]. A large number of fast ion conductors have been developed and used successfully as electrolytes in solid state batteries[4,5]. Batteries fabricated with solid electrolytes can eliminate the problems faced by the liquid electrolytes batteries such as leakage due to corrosion, short shelf life, limitted temperature range of operation, less thermal stability heavy weight, etc[1-3]. Different types of (crystalline, glasses, polymers and composite) superionic conductors with various mobile ions like Li^-, Na^+, Ag^+, Cu^+, Pb^{2+}, etc, have been synthesized and characterized. Among them, silver based glasses show high stability at ambient temperature[2,3,6-8]. Hence, silver based glass solid electrolytes have been synthesized to attain high ionic conductivity[9-10].

We have investigated the conductivity of the glass system (50-x)P_2O_5-xAgI-$40Ag_2O$-$10Fe_2O_3$ [x=0,5,10,15,20,30., by impedance techniqe. Also, we have fabricated the solid state batteries using the highest ionic conductivity glass. Characterization of this battery is performed.

Preparation of samples

The glass system (50-x)P_2O_5-xAgI-$40Ag_2O$-$10Fe_2O_3$ [x=0,5,10,15,20,30., were prepared by melting mixtures of $NH_4H_2PO_4$, AgI, Ag_2O and Fe_2O_3 in the powder form . The mixture was heated in purceline crucbles at a temperature ranging from 250°C to 350 °C for two hours in order to gas evolution ceased . After that, the temperature was raised gradually to 950 °C and left for 6 hours in order to chemical reaction is completed . Then the melt was shaked several times to ensure the homogenity. The melt was poured on a steel plate kept at (0 °C) . Silver paste, which show ohmic contact with glass samples, was used for coating

the desired electrode area . The sample before measurements was left at room temperature for about 10 hrs .

Measurements

Samples of the glass system (50-x)P_2O_5-xAgI-40Ag_2O-10Fe_2O_3 ,[x=0,5,10,15,20,30. were characterized by X-ray diffraction (XRD), Mossbauer effect (ME), infrared (IR) and differential thermal analysis (DTA) measurements. Ac measurements have been carried out in the range of frequency from (500 Hz to 5 MHz) by using a programmable automatic RCL meter (HIOK 3532 LCR HITESTER). The density of studied glasses were measured as a function of AgI content.

Characterization

Glass nature of the prepared samples was confirmed from the peaks free XRD patterns. The structure of each glass sample is confirmed by comparing the observed FT-IR spectral results of our glasses with the reports in the literature[11-13]. Glass transition temperature (Tg) and crystallization temperature (T_c) are identified from the measured DTA curves for the prepared samples. The obtained ME spectra and parameters show that iron exists as Fe3+ occupying both tetrahedral coordination states. It is also found that at high iron oxide content, most of the iron enters the glass network as former while the rest appears as network modifier. In addition a small amount of Fe_2O_3 precipitates which disappears on adding silver oxide.

It is known from the preparation of the glass samples (50-x)P_2O_5-xAgI-40Ag_2O-10Fe_2O_3 , [x = 0, 5, 10, 15, 20, 30. that , AgI increases and P_2O_5 decreases gradually in molecular weight % . This means that , the number of the oxygen decreased gradually when Ag and I are increased. This result confirms the supposition that at low AgI content , the excess oxygen form large non-bridging oxygens as well as the formation of some phosphrous double bond oxygens (P=O)[14]. The disappearance of this bond confirm also the decrease of non-bridging oxygen due to the difficiency of the oxygen anions. In addition, most of iron ions occupy the network forming positions as concluded from both IR and Mossbauer (ME) techniques. Consequently, most of Ag cations prefer to occupy the network modifying positions in the present glass . Increasing AgI content on the expense of P_2O_5 indicates the approximate gradual decrease in the ratio of [(P+Fe)/(O+I). , since Fe acts as a network former . This reavels that , the non-bridging oxygen may decrease while the Ag–P bonds increase. The addition of AgI (increasing silver cations and introducing I anions) may also increase the dangling bonds between I and P or Fe atoms of the form PO_3–I or FeO_3–I. In addition some silver cations may appeared as an isolated (AgI_4) groups.

Density and Molar volume

The density of studied glasses were measured as a function of AgI content . It showed increasing trend in the range from 0 to 20 mole % AgI and appeared to be stable until 30 % AgI . The molar volume (Vm) is calculated. Fig. 1 shows the change in the obtained molar volume values as a function of the AgI content . It is noticed that , as the AgI increased from 0 to 20 mole % , the molar volume decreased linearly , while in the range 20 to 30 mole % AgI , it seems to be stable.

According to the density and the molar volume , the change in their values in the range up to 20 mol % appeared to be small which may reflect the formation of some AgI_4 clusters . The stability of the density and molar volume in the range 20 and 30 % AgI may reflect the stability of the glass network in this range and the increase in silver cations as AgI was gradually increased may lead to increase the P–Ag bonds. The formation of these bonds reflect no change in the network structure of these glasses. This stability was confirmed in agreement with the results of both line width (LW) and quadrupole splitting (QS) values concluded from ME.

From the IR interpretation , the P=O bond at1200 cm^{-1} apperead in the samples contianing AgI from 0 to 10 mole % and disappeared completely in the samples contianing AgI from 15 to 30 mole % . This result confirm the above supposition that at low AgI content , the excess oxygen form large non-bridging oxygens as well as the formation of some phosphrous double bond oxygens (P=O)[11]. The disappearance of this bond confirm also the decrease of non-bridging oxygen due to the difficiency of the oxygen anions

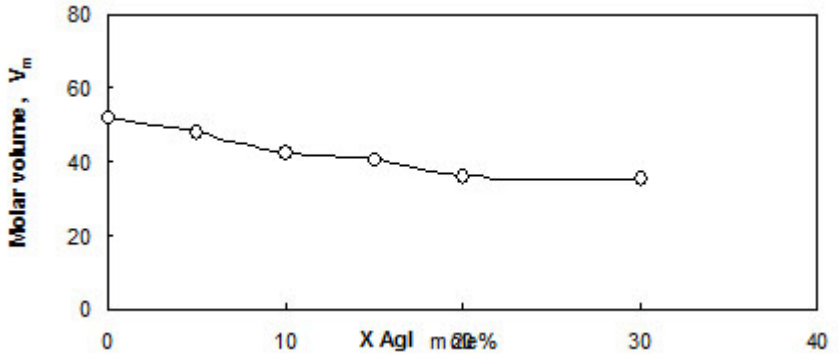

Fig. 1: Relation between Molar Volume (V_m) and xAgI mole% for the glass system (50-x)P_2O_5-xAgI-40Ag_2O-10Fe_2O_3, [x = 0,5,10,15,20,30]

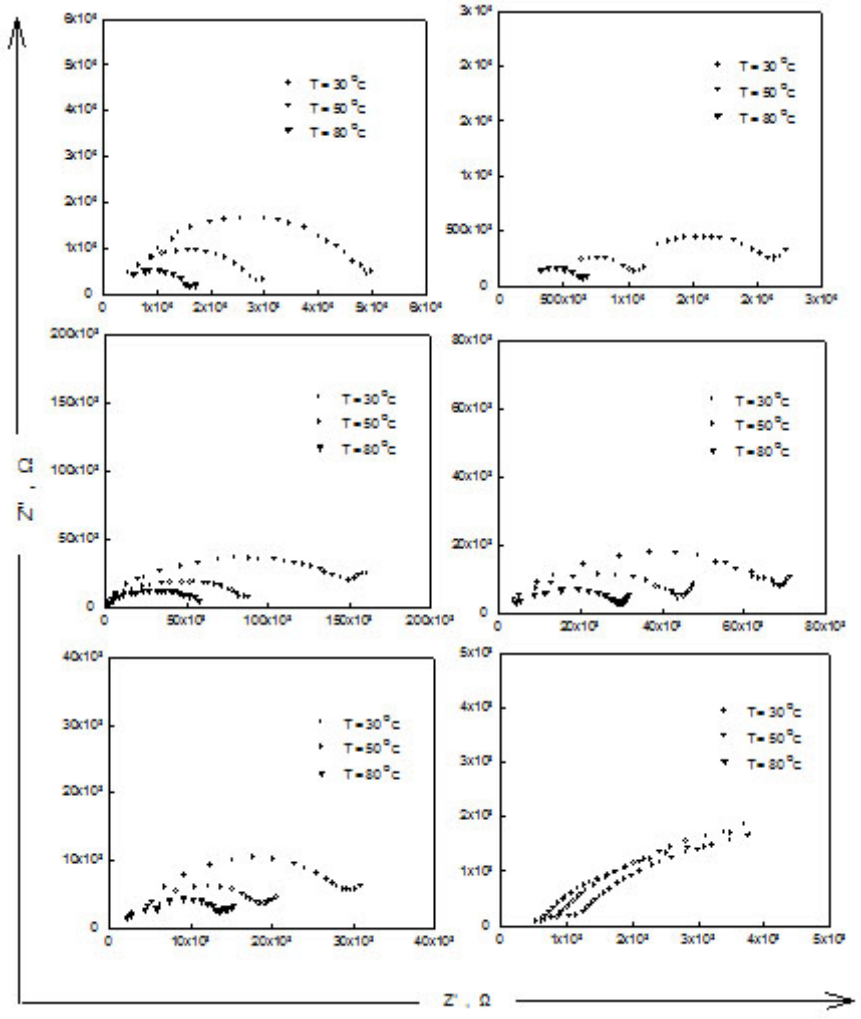

Fig. 2: Plots of Z" vs Z' for the glass system (50-x) P_2O_5-xAgI-40Ag_2O-10Fe_2O_3, [x = 0,5] at different temperatures

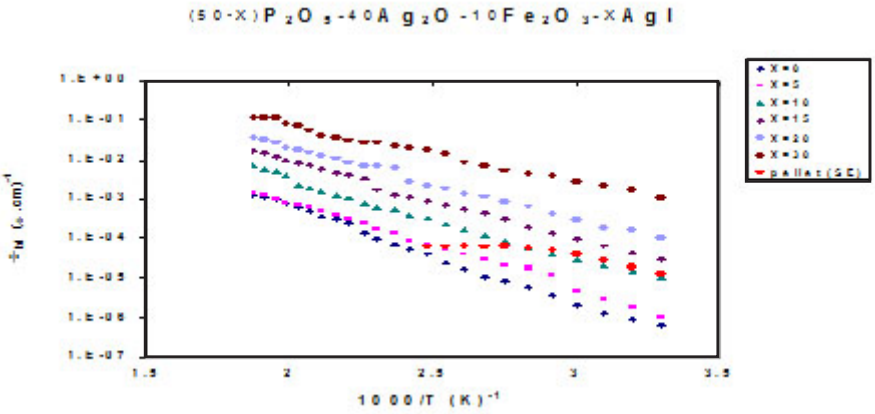

Fig. 3: Temperature dependence of σ_{bl} for the glass system

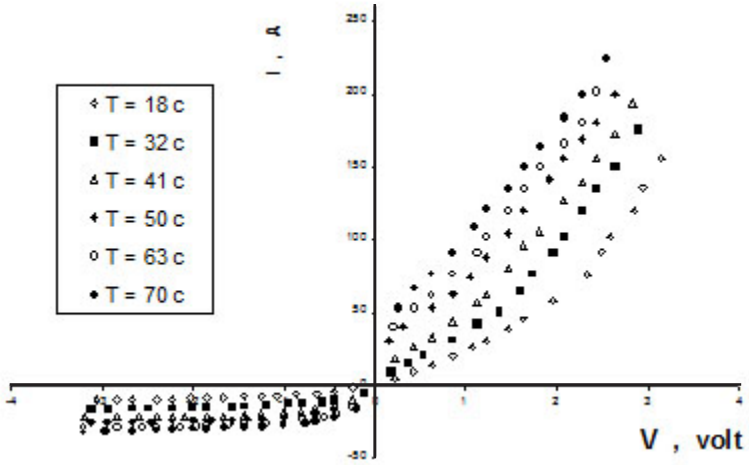

Fig. 4: I-V characterestic curves for the Ag/SE/Ag_2S solid electrolyte in the forward and backward directions

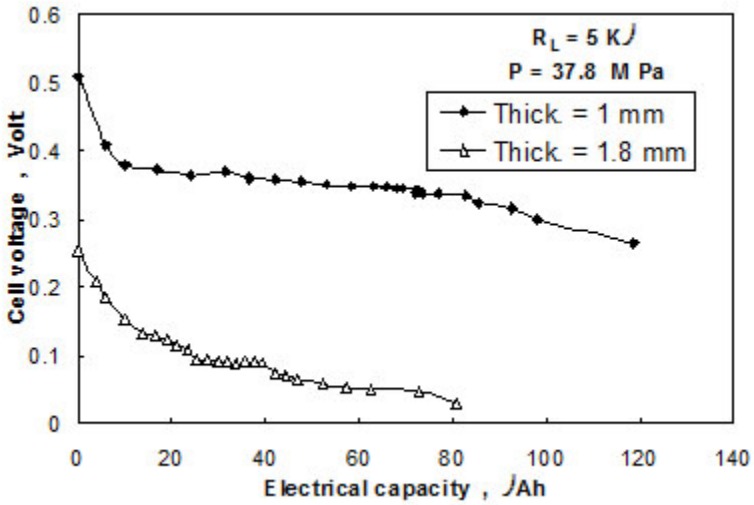

Fig. 5: Cell voltage versus electrical capacity for the solid electrolyte battery Ag/SE/Ag_2S

Electrical Conductivity

The bulk conductivity for the glass system,$(50-x)P_2O_5$-xAgI-$40Ag_2O$-$10Fe_2O_3$, [x=0,5,10,15,20,30.,was estimated using the complex impedene method[15] in the range between room temperature and 500 K and the frequency range (50Hz–5MHz). From fig. 2, the intersection of the semicircle with Z'axis gives the bulk resistance R_{bl} from which bulk conductivity σ_{bl} (σ_{bl} = C *1/R_b , where C is a geometrical constant) can be obtained. The values of σ_{bl} illustrate an increase with increasing AgI content, they also illustrate thermal activation with increasing temperature and obeys Arrhenius equation;

$$\sigma_{bL}T = A \exp(-E_{bL} / KT) \quad ...(1)$$

where E_{bL} is the apparent activation energy obtained using semilogarithmic plot of $s_{bl}T$ versus $10^3/T$, fig. 3. The activation energies are determined and listed in Table 1. It is also noticed that , the activation energy E_{bl} decreases with increasing the xAgI content.

The thermal activation of bulk conductivity (σ_{bl}) with increasing temperature can be interpreted by a structural model which was suggested by T. Minami [16]. This model suggested the occurance of Ag^+ ions with different mobilities in AgI-based superionic glasses in three types of Ag^+ ions: (i) Ag^+ ions are bonded to the oxygen atoms of the network, (ii) Ag^+ ions interact weakly with the network oxygen atoms and (iii) Ag^+ ions are surrounded by I^- ions only. Silver ions of the last type have maximum mobility and contribute mostly to ionic conduction. When the temperature was increased to higher values, the conductivity reaches to higher values because of Ag^+ ions (which interact weakly to the oxygen atoms of the network) may release and contribute in conduction with the Ag^+ ions (which surrounded by I^- ions) leads to increase the concentration of Ag^+ mobile ions.

Solid State Batteries

The high ionic conducting glass $20P_2O_5$-$30AgI$-$40Ag_2O$-$10Fe_2O_3$ was used as a solid electrolyte.The solid electrolyte glass was pulverized into very small grain sizes . The powder was pressed under the desired pressure to obtain pellet of 12 mm diameter and 1 mm thickness . The blocking electrode material is Ag_2S where was mixed with electrolyte glass powder in a weight ratio of 2 : 3 [17.. It was pressed together with the solid electrolyte layer into a two-layered pellet as a positive electrode. Silver paste, which showed ohmic contact with solid electrolyte layer, used to coating the surface of the solid electrolyte layer as a negative electrode. The following type of primary battery: anode / solid electrolyte / cathode is fabricated ((Ag_2S + SE)/solid electrolyte / Ag)

I-V characteristic of the superionic solid electrolyte (SE)

In the present section , it is interesting to study I-V characterestic relationships by using asymmetrical electrodes for the present glass electrolyte (Ag/SE/Ag_2S) , Ag_2S electrode forms blocking. Fig. 4 illustrates a plot of current I against voltage V in the forward and backward direction at different ambient temperatures. The I-V characterestic relationships showed that a production of depletion region arround the interface. The main part of depletion region arised at SE side which forms Schottky diode.

In the absence of any external field on Ag/SE/Ag_2S , the charge carrier density gradient at both sides arround the SE - Ag-$_2S$ interface results in a self diffusion of the majority carriers producing a depletion region at the interface. The main part of the depletion region arised at SE side.The potential barrier arised at interface is attributed to the present of the negative fixed ions inside SE and we neglect the depth of depletion region in Ag_2S side because of its high concentration of charge carriers (=$1x10^{22}$ cm^{-3}).The generation of PO_4^- groups in SE is due to break of O-Ag bonds and consequently a reduction reaction occurs as follows ;

$$Ag^+ + e^- \rightarrow Ag \text{ (Reduction)}$$

The electrons which attack silver ions at SE side generates from oxidation reaction at Ag_2S side as follows ;

$$S^{2-} \rightarrow 2e^- + S \text{ (Oxidation)}$$

The built-in potential height (V_{bi}) arised at Ag_2S-SE interface can be expressed by the following equation [18.;

$$V_{bi} = \frac{KT}{q} Ln \frac{N_{SE}}{N_{Ag2S}} \quad ...(2)$$

where N_{SE} , $N_{Ag2S(electrode)}$ are the concentration of charge carriers of solid electrolyte and Ag_2S electrode respectively. The value of V_{bi} has been estimated using N_{SE}(=1.8×10^{21} cm^{-3}) and

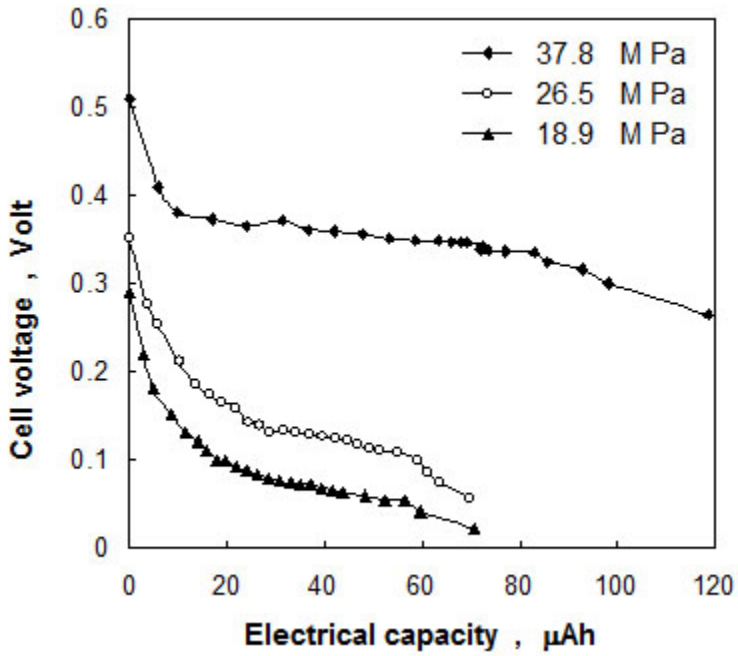

Fig. 6: Cell voltage versus electrical capacity for the solid electrolyte battery Ag/SE/Ag_2S discharged at a constant load resistance 2 MΩ

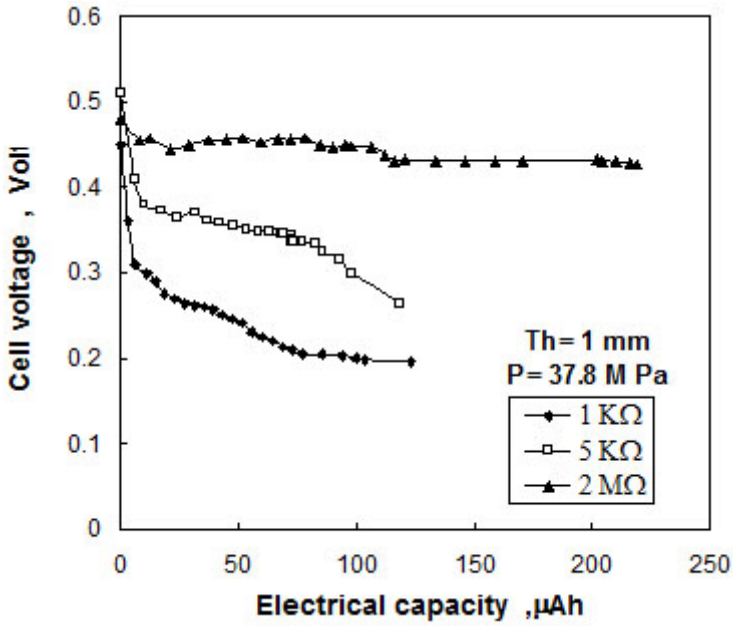

Fig. 7: Cell voltage versus electrical capacity for the battery Ag/SE/Ag_2S discharged at a different load resistances

N_{Ag2S}(=1×10^{22} cm^{-3}) [19.. It is noticed that , the estimated value of V_{bi}(=0.061 eV) is lower than the value of the barrier hight from solid electrolyte to Ag_2S electrode (ϕ_B = 0.082 eV).

Charge and discharge characteristics

The first parameter to be measured to test the fabricated cell is its open circuit voltage (OCV).The cell voltage was measured under no load condition.A voltage of 680mV is found which is very close to the theoretical OCV (687 mV) of the silver based cells with iodine as cathode[20].

The study of the effect of thickness on the

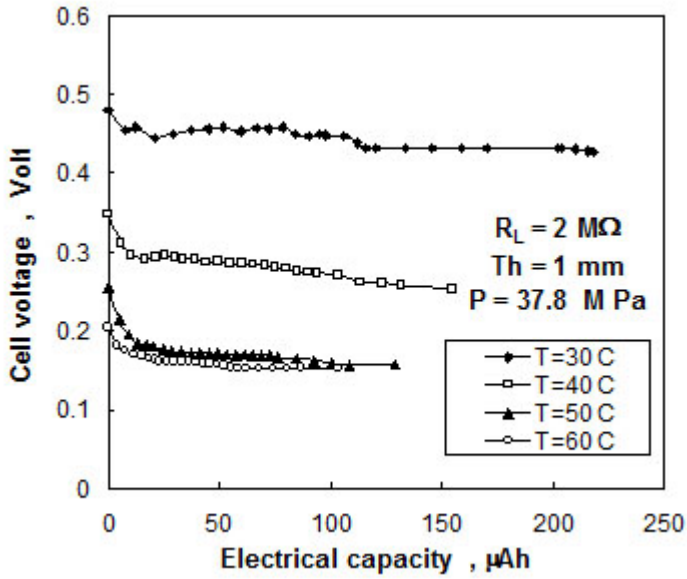

Fig. 8: Cell voltage versus electrical capacity for the solid electrolyte batteryAg/SE/Ag_2S

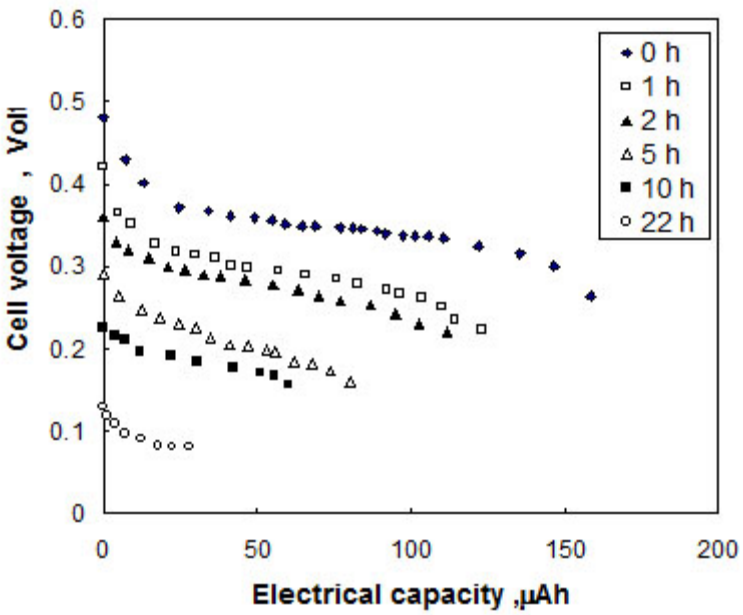

Fig. 9: Cell voltage versus electrical capacity for the solid electrolyte battery Ag/SE/Ag_2S discharged at a constant load resistance 2 MW

charge-discharge processes of the solid electrolyte Ag/SE/Ag_2S battery was performed at room temperature (30 ^oC). Fig. 5 illustrates the cell voltage of the solid electrolyte Ag/SE/Ag_2S battery versus electerical capacity [Q=I × t mAh.[21] at load resistance equal to 5KW . It is noticed that , the cell voltage decreases , in general , to nearly stationary value. It is also noticed that, as the electrolyte thickness increases the cell voltage decreases because of resistance reduction due to the sample thickness decrease leading to an facilitate polarization and/or silver ion migration in the charging process. Consequently this leads to an increase of depelation region at the interface.

The effect of pressure on the charge-discharge process of the solid electrolyte Ag/SE/Ag_2S battery, prepared under different pressures and constant thickness equal to 1mm, was performed at room temperature (30°C). Fig. 6 illustrates the cell voltage against elecrical capacity of the solid electrolyte Ag/SE/Ag_2S battery by using load resistance of 2 MW . It is noticed that, the general behaviour of the cell voltage-electric capacity relation shows a slight decrease of the value of discharge voltage down to stationary value. In addition , the value of cell voltage increases with increasing pressure of preparation .

In the present section we study the effect of load resistance[22] on the cell voltage and discharge current at room temperature (30°C). Fig. 7 illustrates the cell voltage against the electrical capacity for the solid electrolyte Ag/SE/Ag_2S battery at different load resistances . It is noticed that, as the load resistance increases the cell voltage shifts upward . This can be attributed to the load resistance control of the battery current drain. It is also noticed that, the value of electrical capacity in the case of 2MW is higher than that in the case of 1 and/or 5KW because at higher load resistance, 2 MW , the discharge current spend long time at higher values in the whole range of discharge time.

Table 1: The values of Tg, Tc and Ebl for the glass system (50-x)P_2O_5-xAgI-40Ag_2O-10Fe_2O_3,[x=0,5,10,15,20,30]

x AgI	Tg K	Tc K	Ebl
0	375.89	761.12	0.488
5	371.14	754.96	0.432
10	365.76	725.26	0.397
15	360.27	715.82	0.393
20	359.55	613.32	0.366
30	356.81	528.05	0.282

The charge-discharge processes of the solid electrolyte Ag/SE/Ag_2S battery was carried out at different ambient temperatures. Figure (8) illustrates the cell voltage against the electric capacity for the solid electrolyte Ag/SE/Ag_2S battery at different ambient temperatures by using a load resistance equal to 2MW. It is noticed that, discharge voltage decreases slightly to stationary value.In addition the behavior shifts down by increasing ambient temperature.

The discharge processes[17] of the solid electrolyte Ag/SE/Ag_2S battery was performed after different storage times at room temperature. Fig. 9 illustrates the cell voltage against elecrical capacity of the solid electrolyte Ag/SE/Ag_2S battery by using load resistance equal to 2MW. It is noticed that , the cell voltage shows remarkable decrease down to stationary value . It is also noticed that , the values of cell voltage decreases as the storage time increased which can be attributed to the charge leakage (recovery process) .

CONCLUSIONS

The results of superionic solid electrolyte glass for chargeable battery application at different coditions showed that :-

- The high ionic conducting glass 20P_2O_5-30AgI-40Ag_2O-10Fe_2O_3 was used as a solid electrolyte.
- The I-V characterestic relationships , for the superionic solid electrolyte powder using asymmetric electrodes at forward and backward direction, showed that a production of depletion region arouned the interface.
- The charging and discharging of solid electrolyte battery (Ag/ SE/ Ag_2S) is reproducible. The leakage of stored charge is greatly dependent on, time of storage, ambient temperature and device preparation conditions.

REFERENCES

1. S. Chandra, Super ionic Solids: Principal and Applications, North- Holland Publications, (1981).
2. W. Van Gool (Ed.), Fast Ion Transport in Solids, North- Holland Publications (1973).
3. B.V.R. Chowdari and S. Radhakrishna (Eds.), Solid State Ionic Devices, World Scientific & Co., (1988).
4. R.T. Foley, *J. Electrochem. Soc*., 13c (1969).
5. K. Shahi, J.B. Wagner and B.B. Owens, in: J.P. Gabano (Ed), Lithium Batteries, Academic Press, NY, 407 (1983).
6. C.A. Vincent, *Prog. Solid State Chem*. **17**: 145 (1987).
7. P.Mcgeehin and A. Hooper, *J. Mater. Sci.* **12**: 1 (1987).
8. T. Minami, *J. Non-Cryst. Solids* **73**: 273 (1985).
9. B.B. Oowens, *Adv. Electrochem. Eng*. **8**: 1 (1971).
10. R. Patcheammalle, Ph.D thesis. Pondicherry University, India (2000).
11. S. Jayaseelan, N. Satyanarayana and M. Venkateswarlu, *J. Mater. Sci. Eng*. B**106**: 46 (2004).
12. S. Jayaseelan, N. Satyanarayana and M. Venkateswarlu, *J. Mater. Sci*. **39**: 1717 (2004).
13. S. Jayaseelan, N. Satyanarayana and M. Venkateswarlu, *Mater. Chem. Phys*. **87**(2-3): 370 (2004).
14. J.P. Malugani, R. Mercier, B. Fahys and G. Robert**,** *J. Sol. State Chem.*, **45**: 309 (1982).
15. J.E.Bauerle*, J. Phys. Chem. Solids*, **30**: 2657 (1969).
16. T. Minami**,** *J. of Non-Crystalline Solids* **56**: 15-26 (1983).
17. K. Iwamoto, N. Antoni, K. Takada and S. Kondo, *Solid State Ionic* **79**: 288 (1995).
18. S.M.Sze**,** "Physics of Semiconductor Devices" , John Wiley & Sons , Inc. (1969).
19. D.P.allmond , G.K.Duncan and A.R.West*, Solid State Ionics*, **8**: 58 (1983).
20. T. Takahashi and O. Yamammto, *J. Electrochem*. **116**: 95 (1974).
21. K. Takada, N. Antoni, K. Iwamoto and S. Kondo, *Solid State Ionic* **86-88**: 288 (1996).
22. R. C. Agrawal and R. Kumar, *J. Phys. D: Appl. Phys*. **27**: 2437 (1994).